A study of uranium-based multilayers: I. Fabrication and structural characterization

2008 J. Phys.: Condens. Matter 20 215229

(http://iopscience.iop.org/0953-8984/20/21/215229)

J. Phys.: Condens. Matter **20** (2008) 215229 (8pp) doi:10.1088/0953-8984/20/21/215229

A study of uranium-based multilayers: I. Fabrication and structural characterization

R Springell[1,2], S W Zochowski[1], R C C Ward[3], M R Wells[3], S D Brown[2,4], L Bouchenoire[2,4], F Wilhelm[2], S Langridge[5], W G Stirling[2,4] and G H Lander[6]

[1] Department of Physics and Astronomy, University College London, London WC1E 6BT, UK
[2] European Synchrotron Radiation Facility, BP220, F-38043 Grenoble Cedex 09, France
[3] Clarendon Laboratory, University of Oxford, Oxford OX1 3PU, UK
[4] Department of Physics, University of Liverpool, Liverpool L69 7ZE, UK
[5] ISIS, Rutherford Appleton Laboratory, Chilton, Oxfordshire OX11 0QX, UK
[6] European Commission, JRC, Institute for Transuranium Elements, Postfach 2340, Karslruhe, D-76125, Germany

E-mail: ross.springell@esrf.fr

Received 17 December 2007
Published 25 April 2008
Online at stacks.iop.org/JPhysCM/20/215229

Abstract

This paper addresses the structural characterization of a series of U/Fe, U/Co and U/Gd multilayers. X-ray reflectivity has been employed to investigate the layer thickness and roughness parameters along the growth direction and high angle diffraction measurements have been used to determine the crystal structure and orientation of the layers. For the case of uranium/transition metal systems, the interfaces are diffuse (∼17 Å) and the transition metals are present in a polycrystalline form of their common bulk phases with a preferred orientation along the closest packed planes; Fe, bcc (110) and Co, hcp (00.1), respectively. The uranium is present in a poorly crystalline orthorhombic, α-U state. In contrast, the U/Gd multilayers have sharp interfaces with negligible intermixing of atomic species, and have a roughness, which is strongly dependent on the gadolinium layer thickness. Diffraction spectra indicate a high degree of crystallinity in both U and Gd layers with intensities consistent with the growth of a novel hcp U phase, stabilized by the hcp gadolinium layers.

(Some figures in this article are in colour only in the electronic version)

1. Introduction

The properties of a material can differ greatly from the bulk when reduced in size into the nanometre regime. The fabrication of multilayers results in the juxtaposition of different elements in systems where the interfacial regions comprise a substantial part of the whole sample, producing interesting electronic and magnetic effects [1]. The use of the actinide element uranium in such systems can be used to investigate effects arising from the unpaired 5f electrons, which exhibit strong hybridization with other electronic states in uranium compounds [2].

The overall objective of this research programme is to examine the interactions of the 3d and 4f elements with uranium in the form of multilayers. Because of the extended nature of the 5f electron states in uranium, we expect hybridization at the interfaces between the U 5f states and those of the other element, possibly causing a number of interesting effects, such as observing induced U 5f magnetic moments. Before being able to examine such microscopic interfacial effects, it is necessary to develop growth and characterization methods and understand the average structural and bulk properties of the multilayers and the interfaces. This is the objective of the present papers; later articles will focus on element specific techniques or specifically the interfaces, with transmission electron microscopy. We report experiments on multilayers with Fe, Co and Gd as secondary elements. In these cases, since the elements are ferromagnets, we can

examine also the bulk magnetic properties of the multilayers, with the expectation that modifications of the ferromagnetic properties will reflect both the influences of the structure and/or effects arising from the interaction with the uranium layers. An important consideration in the formation of multilayers is the relative size (atomic volume) of the elements; we note that uranium is intermediate between the small 3d elements and the large 4f elements.

The polarization of uranium was reported in a study of the UAs/Co multilayer system [3, 4], where the proximity of the amorphous ferromagnetic UAs compound to the transition metal (TM) ferromagnet, Co, resulted in a large magneto-optical Kerr effect from the uranium [5]. The first reports of multilayers, including uranium in its elemental form, discuss the proximity effects of the transition metals Co [6] and Fe [7]. Our group has carried out a series of experiments on U/Fe multilayers [7, 8]. These papers discuss the fabrication and characterization of a series of samples, using a combination of x-ray reflectivity, x-ray diffraction, Mössbauer spectroscopy, bulk magnetization and polarized neutron reflectivity (PNR) techniques. Since these studies, modifications to the sputtering apparatus at the Clarendon laboratory, Oxford, have improved the control of the sputtering rates and the inclusion of a third sputter-gun has allowed the growth of buffer and capping layers to seed the crystalline assembly of the bilayers and prevent oxidation of the multilayer stack. Recent measurements of the x-ray magnetic circular dichroism (XMCD) at the U M-edges have probed the electronic behaviour of the U 5f states in U/Fe multilayers [9] and confirmed earlier x-ray resonant magnetic reflectivity (XRMR) measurements [10], which demonstrate that a polarization of the uranium 5f electrons occurs in the U/Fe multilayers as a result of the hybridization of (U)5f–3d(Fe) electrons.

In the present articles (I and II), we report on a new series of U/Fe multilayers and extend our study to the transition metal U/Co system. In addition, the fabrication and characterization of a series of U/Gd multilayers is also described. In order to understand the growth mechanisms and structural properties of this range of systems, it is helpful to recall the sizes of the respective atoms. The atomic volumes of Fe and Co are $\sim$12 Å^3, whereas that of U is $\sim$21 Å^3, assuming the latter to be in the room temperature, ambient form of the alpha phase, which has an orthorhombic crystal structure. The resulting mismatch in one dimension is $\sim$20% and would result in a considerable compressive strain on the uranium. In contrast, the atomic volume of Gd is $\sim$33 Å^3, giving a length mismatch of $\sim$14% and a strain that is clearly in the opposite sense to that found when using 3d transition metal elements. These strains could result in significantly different structural and magnetic properties between the U/TM and U/Gd multilayers.

2. Fabrication

Multilayers were fabricated using a three-gun, dc magnetron sputtering assembly in a loadlocked growth chamber operating at UHV base pressure (5×10^{-10} mbar). Substrates were single crystal sapphire plates, which were epi-polished parallel to the (11.0) plane. A 50 Å thick niobium buffer layer was used to seed crystalline growth of the bilayers. Nb has a body centred cubic (bcc) crystal structure and is expected to exhibit [110] preferred orientation on sapphire (11.0) when deposited at ambient temperature (it is fully epitaxial at elevated temperature). A similar Nb layer was used as a capping layer to prevent atmospheric attack of the multilayer after growth. A study of epitaxial (110) Nb films on sapphire has found that a stable layer of Nb_2O_5 about 20 Å thick is formed, which provides effective long-term passivation [11].

Sputtering was carried out in a (flowing) argon pressure of 5×10^{-3} mbar, and a growth rate $\sim$1 Å s^{-1} was employed for each element. Precise deposition rates were determined from measurement of calibration samples, by comparison of experimental and calculated x-ray reflectivity profiles. The majority of samples were grown at ambient temperature, although a substrate heater was available to investigate the effects of elevated temperature on selected samples.

3. Structural characterization

Series of U/Fe, U/Co and U/Gd samples were made in order to study the structural properties systematically as a function of the layer thicknesses of the respective elements, and to contrast and compare trends between the systems. The samples were grown with layer thicknesses in the ranges $5 < t_U$ (Å) < 90 and $10 < t_M$ (Å) < 80, where t_M is the ferromagnetic element.

The x-ray reflectivity technique was employed, using a Cu Kα source, to investigate the composition of the multilayers in terms of the layer thickness and interface roughness values [12]. This technique provides an excellent measure of the bilayer thickness, but is limited in its sensitivity to the relative thicknesses of individual layers. The reflectivity was calculated using the xPOLLY programme [13]. A set of input parameters was used, including the anomalous scattering factors of the respective materials at the energy of the incident photons, the density (atoms Å^{-3}), the layer thickness (Å) and the rms roughness (Å). All of these values can be varied, although in practice the scattering factors were kept constant and the structural parameters varied. The initial structural models consist of a substrate, Nb buffer layer, repeated bilayer and an oxidized capping layer. Complexity can then be introduced by stratifying the bilayer to account for regions of reduced density at the interfaces, where strain, caused by lattice mismatches between relevant species, can produce defects affecting the crystal structure of the layers.

Good fits to the data could be produced with individual layer thicknesses varying by several angstroms. For this reason, the reflectivity was not considered in isolation, but consistency was maintained by consideration of the growth parameters and results from x-ray diffraction, PNR and SQUID magnetometry measurements [14]. High angle x-ray diffraction measurements were used to investigate the crystal structures of the respective elements within the layers.

3.1. X-ray reflectivity

The results are presented for the specular reflectivity of U/Fe, U/Co and U/Gd systems respectively. This scattering geometry

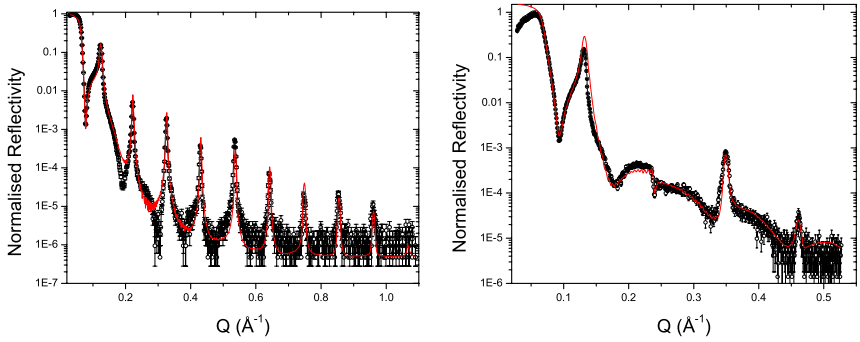

(a) SN74 – $[U_{32}/Fe_{27}]_{30}$ (b) SN108 – $[U_{27.5}/Co_{27.5}]_{20}$

Figure 1. The normalized reflected intensity is presented as a function of the wavevector momentum transfer, **Q** for selected U/Fe and U/Co samples. Calculated reflectivity curves (solid red line) were fitted to the data (open points) using the xPOLLY programme [13]. Layer thicknesses are as fitted; we note that the precision is of order 1 Å (see text).

probes the reflected intensity as a function of depth, where the x-rays are sensitive to the electron density profile. Figure 1 shows examples of the x-ray reflectivity spectra for U/Fe (a) and U/Co samples (b). The total bilayer repeat distance was determined with a precision of 0.1 Å, but the individual layer thicknesses could not be so well defined. However, restrictions were fixed on these values based on the sputtering times and known calibrations.

The U/Fe samples analysed previous to this work using x-ray reflectivity [7] were grown on glass substrates and did not include either a buffer or a capping layer to prevent oxidation. The use of an Nb capping layer reduces the complicated oxidation profile through the multilayer stack to a Nb/Nb_2O_5 surface layer. This implies a simpler calculation of the reflected intensity and one which includes a similar surface contribution for all of the samples.

The reflectivity results for the U/Co samples were fitted by separating the cobalt layers into two components; one reduced density (>90% of the bulk value) component of ∼15 Å thickness and the remainder of the bulk Co density, $\rho_{Co} = 9 \times 10^{28}$ m^{-3}. This structural profile was determined from the polarized neutron reflectivity and bulk magnetization measurements to be discussed in paper II [14] of this series. It was not possible to identify a U–Co alloy region at the interface as indicated by Mössbauer measurements on U/Fe samples, although it is likely to be present due to the similar atomic sizes of Fe and Co resulting in similar interfacial strains. The majority of the features have been reproduced by the calculations, including the extinction of even order Bragg peaks in the case of sample SN108, figure 1(b), where the thicknesses t_U and t_{Co} are almost equal.

Figure 2 shows representative reflectivity spectra for a range of U/Gd multilayers. Panels (a) and (b) have similar bilayer repeat thicknesses, but vary in composition between thick Gd layers and thick U layers, respectively. The difference in the spectra is striking; for large values of t_{Gd} (a) the reflected intensity decreases rapidly as a function of **Q**, compared with the observation of well-defined Bragg peaks over a wide **Q** range in the reflectivity spectra of samples with thick U layers, e.g. (b). Graphs (a) and (c) show the reflectivity curves for samples of decreasing Gd layer thickness for almost constant values of t_U and indicate a reduction in the bilayer roughness for thin Gd layers. Figure 2(d) contrasts the reflectivity spectrum observed for a U–Gd alloy sample with those of U/Gd multilayers.

3.1.1. Discussion. The general good quality of multilayer samples in all cases is supported by the form of the measured x-ray reflectivity profiles. The relative growth properties of U/Fe samples grown on sapphire substrates with niobium buffer and capping layers can be compared to those grown previously on glass with no buffer or capping layers [7], by comparing relative thickness and roughness parameters. The roughness of layers in the latter, although ∼1–2 Å larger for samples of similar layer thickness, are of approximately the same magnitude, indicating that the bilayer growth mechanisms are the same in both cases and that the majority of the roughness stems from the relative lattice mismatch and crystalline nature of the respective species. The slightly reduced roughness in the new samples can be understood as an effect of the smooth substrate surface and low roughness value of the niobium buffer layer.

Both U/Fe and U/Co samples were modelled by separating the ferromagnetic layers into two components; one with a reduced density (10% less than the bulk value), ∼15 Å thick, and the remainder of the layer with the bulk density. This model is supported by results obtained in PNR, Mössbauer and SQUID magnetometry [7, 8] measurements, discussed in paper II [14], and can be understood by considering the growth of layers with a large mismatch in lattice spacings, ∼20%. The large strains and diffusion of the smaller transition metal atoms into the uranium layers produce an alloyed region at the interfaces. Growth of the ferromagnetic layers onto these alloys produces an initial amorphous, noncrystalline form, but as the layer thickness is increased the layer tends towards a bulk crystalline state.

All uranium/gadolinium samples were modelled with a simple bilayer structure, since magnetization measurements [14] have not revealed the presence of any substantial 'dead' layer, requiring a stratified density gadolinium layer. As shown in figure 2 and table 1, for thick uranium layers a large number of Bragg peaks were observed over a wide **Q**-range,

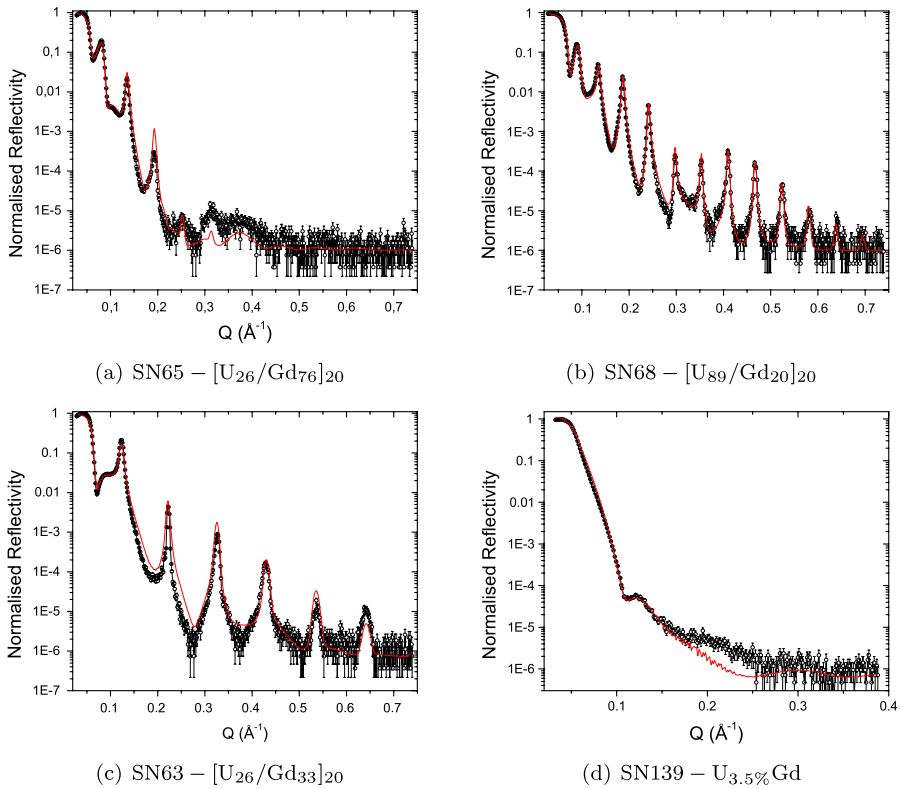

(a) SN65 – $[U_{26}/Gd_{76}]_{20}$ (b) SN68 – $[U_{89}/Gd_{20}]_{20}$

(c) SN63 – $[U_{26}/Gd_{33}]_{20}$ (d) SN139 – $U_{3.5\%}Gd$

Figure 2. U/Gd x-ray reflectivity spectra taken at room temperature. Calculated reflectivity curves are shown as solid red lines. Note that the sample SN139 shown in panel (d) is not a multilayer, but a sputtered alloy of ∼3.5% U in Gd.

Table 1. Roughness values per layer (Å ± 10%) as a function of (a) gadolinium thickness and (b) uranium layer thickness.

Sample	Composition	σ_U	σ_{Gd}	σ_{av}
	(a)			
SN63	$[U_{26}/Gd_{33}]_{20}$	3.2	7.0	5.1
SN64	$[U_{26}/Gd_{54}]_{20}$	7.0	7.0	7.0
SN65	$[U_{26}/Gd_{76}]_{20}$	9.0	10.0	9.5
	(b)			
SN66	$[U_{39}/Gd_{20}]_{20}$	3.0	5.0	4.0
SN67	$[U_{63.5}/Gd_{20}]_{20}$	3.2	5.5	4.4
SN68	$[U_{89}/Gd_{20}]_{20}$	2.9	5.0	4.0

characterized by a low rms roughness of ∼4 Å per layer. For an equivalent bilayer thickness, but with thick gadolinium layers, the roughness was larger, possibly caused by a more columnar crystal growth, resulting in a step-like roughness profile. The large difference between the x-ray reflectivity in these two cases was not apparent for similar situations in the U/Fe and U/Co systems.

Tables 1 (a) and (b) show the rms roughness values for a selection of U/Gd samples; a set with constant t_U and increasing t_{Gd} and a series with constant t_{Gd} and varying t_U. Average roughness values are given in Å for the uranium (σ_U) and gadolinium (σ_{Gd}) layers, and σ_{av} represents an average roughness per bilayer. Similar to the determination of individual layer thicknesses from the simulation of the x-ray reflectivity spectra, the individual layer roughnesses were also difficult to distinguish precisely, although the intensities were very sensitive to σ_{av}. However, the vast majority of samples studied indicated larger roughness values for the gadolinium layers than for the uranium. Table 1 (a) shows a near linear relationship between t_{Gd} and σ_{av}, where thicker Gd layers result in large rms roughness values. In contrast, table 1 (b) shows a practically constant σ_{av} for a range of U layer thicknesses.

3.2. X-ray diffraction

The previous section has dealt with the use of x-rays to probe the physical composition of the multilayers on length scales of order 10–1000 Å, perpendicular to the plane of the sample. It is also important, however, to be able to determine the crystal structure and orientation of the respective layers and various properties of the crystallites that have formed. A study of this type gives insight into the growth mechanisms and interfacial structure of the multilayer samples. X-ray diffraction is the most commonly used and readily available tool for the investigation of these properties.

Due to the lattice mismatch between the respective elements in the case of U/TM and U/Gd systems the samples considered here are likely to be composed mainly of polycrystalline layers with a preferred orientation and a range of crystallite sizes.

3.2.1. Results. The results are presented for the x-ray diffraction in a θ–2θ geometry for U/Fe, U/Co and U/Gd systems, respectively. Summaries of the x-ray diffraction

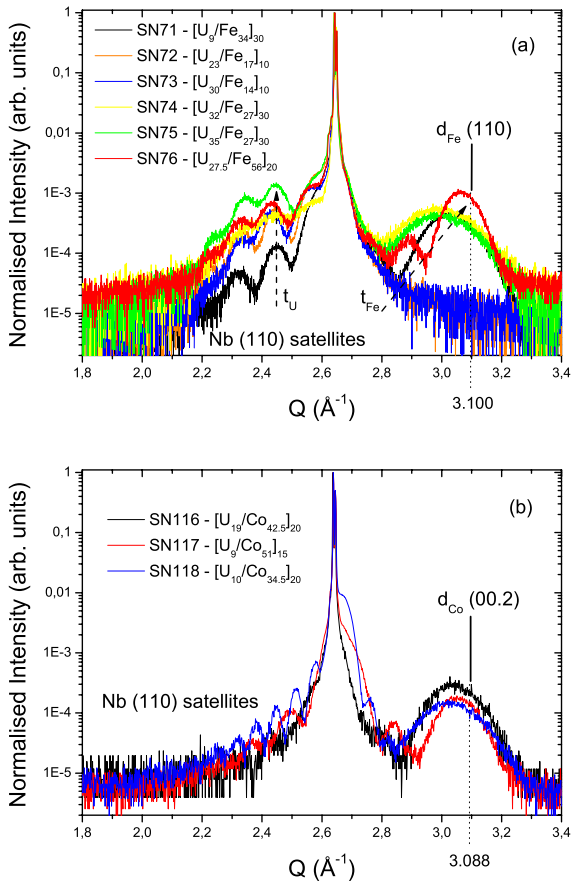

Figure 3. Comparison of the x-ray diffraction patterns close to the sapphire (11.0) peak, for selected U/Fe samples (upper panel) and selected U/Co samples (lower panel). The arrows in panel (a) indicate increasing U and Fe layer thicknesses. The d-spacings of Fe (110) and Co(00.2) are indicated.

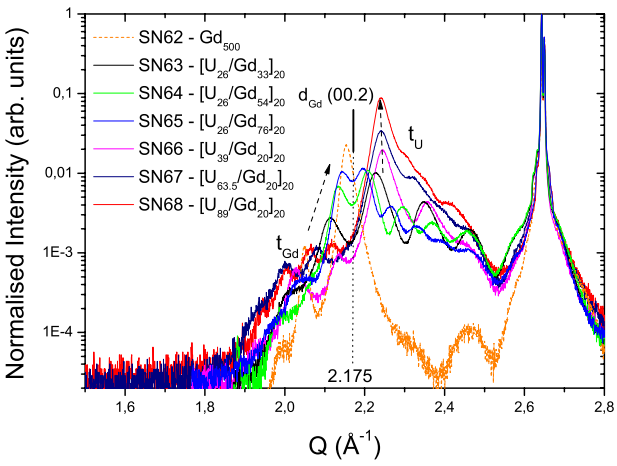

Figure 4. Comparison of the x-ray diffraction patterns close to the sapphire (11.0) peak, for a series of U/Gd samples. The dashed orange curve represents the diffraction from a 500 Å thick sputtered Gd film, which results in a lattice spacing, d_{Gd} of 2.92 Å. The position of the bulk values is also noted.

Table 2. Lattice spacings ($d_{Fe,Co}$) and particle sizes (D) of Fe and Co layers for a selection of U/Fe, U/Co samples, determined by an investigation of the diffraction peak positions and widths, using the Scherrer formula. For bulk bcc Fe $d_{(110)} = 2.027$ Å and for bulk hcp Co $d_{(00.2)} = 2.035$ Å.

Sample number	Composition	$d_{Fe,Co}$ (Å $\pm$ 0.005)	D (Å $\pm$ 2)
SN71	$[U_9/Fe_{34}]_{30}$	2.052	31.0
SN74	$[U_{32}/Fe_{27}]_{30}$	2.073	23.5
SN75	$[U_{35.2}/Fe_{27}]_{30}$	2.073	23.1
SN76	$[U_{27.5}/Fe_{57}]_{30}$	2.045	49.4
SN116	$[U_{19}/Co_{42.5}]_{20}$	2.064	28.3
SN117	$[U_9/Co_{51}]_{15}$	2.058	43.2
SN118	$[U_{10}/Co_{34.5}]_{20}$	2.075	31.7

patterns for U/Fe and U/Co systems are presented in figures 3(a) and (b), whereas figure 4 summarizes the series of U/Gd samples. The diffracted intensity is plotted against the momentum transfer, **Q** (Å^{-1}), for each series of samples in order to compare qualitatively structural variations of the properties across the series. The intensity is normalized to unity at the peak of the scattering from the sapphire substrate.

The upper panel of figure 3 shows a summary of the x-ray diffraction patterns taken for the U/Fe series of samples. The intense peak at 2.643 Å^{-1} is due to the epitaxial sapphire substrate and the satellite peaks that appear on the low angle side of the substrate peak are a consequence of the ∼50 Å thick niobium buffer layer. The α-uranium (110), (021) and (002) peaks were observed previously in diffraction spectra of U/Fe multilayers grown on glass [7] and are positioned at 2.448 Å^{-1}, 2.490 Å^{-1} and 2.537 Å^{-1}, respectively. In our case, these peaks cannot be observed due to the presence of the Nb buffer diffraction peaks, whose intensity is a consequence of the crystalline quality of the niobium layer. However, it is possible to see an increase in the background intensity at the α-uranium peak positions, dependent on the thickness of the uranium layers.

The broad hump on the high angle side of the substrate peak is close to the bulk bcc (110) iron position and there are no other peaks corresponding to bcc Fe, suggesting a preferred orientation in this growth direction. This confirms predictions considering only the likely growth in the direction of the most closely packed planes. The lack of any intensity for iron layer thicknesses of <20 Å suggests that this represents a crystalline limit, below which the growth would be expected to be amorphous and consequently of reduced magnetization. The positions of the iron peaks were used to deduce values for the average lattice spacing in the growth direction, d_{Fe}, and the mean crystallite size, D, was determined by measuring the width of the peaks and using the Scherrer equation [15]. As the diffracting volumes become smaller the peaks broaden, giving a finite $\Delta\theta$ width. The size of the diffracting particles, D, is given by $D = \frac{K\lambda}{\Delta\theta \cos\theta_B}$, where $K = 0.9394$ and θ_B is the Bragg angle [15]. Values for d_{Fe} and D, determined by this method are given in table 2 for a selection of U/Fe samples.

The average lattice spacings are larger than the bulk Fe value of $d = 2.027$ Å, indicating an overall lattice expansion. As the thickness of the iron layer is increased the lattice spacing approaches that of the bulk value for a bcc ([110] oriented) crystal. The particle size scales with Fe layer thickness, but is

several Å thinner than the Fe layers. This is consistent with the picture of a non-coherent growth between the α-U and Fe atoms; crystallites do not extend across more than one layer due to the poor registry between Fe and U crystal planes and regions of alloy at the interfaces.

The lower panel of figure 3 shows a summary of the x-ray diffraction patterns taken for several U/Co samples. The changing period of the niobium satellites can be seen on the low angle side of the sapphire substrate peak as the buffer thickness is changed; SN117 has ∼50 Å Nb and SN118, ∼100 Å Nb. It was not possible to see any effect of varying t_U on the observed diffracted intensity. The diffraction patterns for the U/Co series of samples are remarkably similar in character to those of the U/Fe system, since the position of the hcp (00.2) cobalt peak lies at almost exactly the same wavevector as that for bcc (110) iron. The nature of the broad hump on the high angle side of the substrate peak is influenced by the thickness of the cobalt layers and a similar relationship can be observed between t_{Co} and the diffracted intensity of the cobalt layers, as was seen for the U/Fe series of samples.

The observed intensity of the cobalt hcp (00.2) peak, whereas no other peaks are observed at other allowed hcp Co crystallographic directions, indicates a preferred orientation in this growth direction, expected since it is the most closely packed plane within the hcp crystal structure. The average particle size, D, and the lattice spacing, d_{Co}, were determined, using the same method outlined for the U/Fe samples, and these are summarized in table 2.

Samples SN117 and SN118 (see figure 3 (lower panel) and table 2) were grown at an elevated substrate temperature of ∼450 K. For all U/Co samples, the particle sizes follow a similar trend to that observed for the U/Fe system, although the crystallite sizes are larger in proportion to the Co layer thicknesses for the samples grown at elevated temperature. As for the U/Fe samples, the lattice spacings are expanded compared to the bulk, but tend towards the bulk value as t_{Co} increases. The use of the Scherrer equation to extract a particle size is standard practice, but the broadening of the peaks may be due to other causes, such as lattice strains and microstructural effects. In our case, the fact that the particle size increases as the substrate temperature increases is reassuring; increased thermal energy during the deposition process would, for example, be expected to reduce the dislocation density.

Figure 4 shows a summary of the x-ray diffraction patterns taken for a series of U/Gd samples. There are a number of striking differences in the form of the diffracted intensity between the U/TM and the U/Gd multilayers. The multilayer diffraction peaks occur on the low-**Q** side of the sapphire substrate peak and their intensity reaches values up to one tenth of the intensity of the substrate peak, more than two orders of magnitude larger than the intensity observed for the U/Fe and U/Co systems. This indicates a far greater degree of crystallinity for the U/Gd than for the U/TM samples. The diffraction satellites from the highly crystalline niobium buffer layers are not observable in most cases above the multilayer diffraction peaks, although a contribution from the niobium can be observed as a shoulder on the low angle side of the substrate peak. A gadolinium film (SN62) of ∼500 Å was grown to confirm the expected position of the diffraction peaks in the multilayer samples and diffraction data for this sample are shown as the dashed curve in figure 4.

The series of U/Gd multilayers of figure 4 was grown to investigate the relationship between t_{Gd} and t_U on the structural and magnetic properties of the U/Gd system. The accepted values for the lattice parameters of the hexagonal close packed crystal structure of gadolinium are $a = 3.631$ Å and $c = 5.777$ Å, giving a contraction from the hard sphere model for the c/a ratio (1.633) to 1.591. In these measurements we are sensitive only to length scales in the z-axis direction, perpendicular to the plane of the film, so our discussion will centre around the c-axis lattice parameter and the lattice spacings.

In the case of the single film of gadolinium the (00.2) peak is centred at a **Q** value of 2.152 Å^{-1}, corresponding to a c-axis lattice parameter of 5.840 Å, an expansion from the bulk of about 1%. It is also possible to observe intensity from the niobium buffer at 2.450 Å^{-1} and a peak at 2.040 Å^{-1}, corresponding to the hcp (10.0) reflection that occurs in the bulk at 1.998 Å^{-1}. Indicated by a dashed arrow on figure 4, as t_{Gd} increases, there is a distinct increase in intensity of one of the component peaks in the diffraction patterns, close to the hcp (00.2) peak observed for the thin Gd film. This increase is accompanied by a shift in position from the low angle side of the (00.2) peak towards the thin film value, indicating a lattice expansion for thinner Gd layers.

As the uranium layer thickness, t_U, is varied there is a clearly visible increase in the intensity of one of the component peaks in the x-ray diffraction spectra, at 2.245 Å^{-1} for SN66, SN67 and SN68. This peak does not relate to any of the known peak positions in the α-U phase, but could correspond to the (00.2) peak of an [00.1] preferred orientation hcp U crystal structure. Recent theoretical and experimental evidence [16, 17] supports the existence of a stable hcp U phase established in thin film structures, for a uranium film grown on a [110] oriented bcc, tungsten single crystal substrate. STM images [16] have described a hexagonal arrangement of atoms with a U–U distance of $a = 3.5 \pm 0.5$ Å, although a previous report by Molodtsov *et al* [17] suggested a U–U distance of 3.2 ± 0.1 Å. A theoretical model [16], employing the local density approximation (LDA), supports the idea that an hcp U crystal structure can be stabilized with a c/a ratio of 1.8, appreciably larger than the hard sphere, hcp model value of 1.633. The predicted values for c and a are 5.35 Å and 2.97 Å, respectively. However, it is accepted that there is a tendency for the LDA theory to over-compress the lattice and the actual values for the c and a lattice parameters may be larger than these values.

Assuming that the uranium stacks along the [00.1] axis, a reflection would be observed in the diffraction spectrum at $\mathbf{Q} \sim 2.3$ Å^{-1}, which is close to the position of the diffraction peak attributed to the uranium in figure 4. Moreover, this peak position results in a lattice spacing along the c-axis only 5% larger than that expected for gadolinium, which could provide the mechanism for the growth and orientation of the exotic hcp phase of uranium.

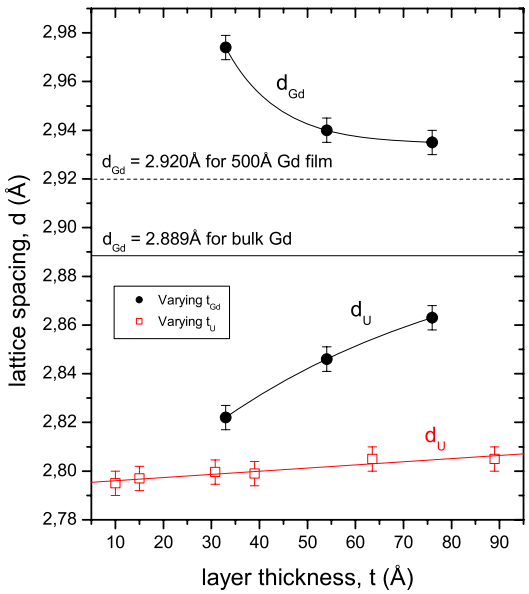

Figure 5. Variations in the lattice spacings of uranium and gadolinium as a function of t_{Gd} (full points) and t_U (open squares) are plotted. Values of the lattice spacing for bulk gadolinium and for a thin Gd film are labelled. Solid lines are guides for the eye.

3.2.2. Discussion. The U/Gd diffraction spectra are markedly different from those observed for the U/TM multilayers investigated thus far. The peaks attributed to the hcp Gd (00.2) and hcp U (00.2) crystalline phases exhibit a mismatch of $<5\%$ in the growth direction, and satellite peaks can be seen either side of the primary ones. This observation is suggestive of a coherent growth of U and Gd layers, giving coherent scattering from crystalline planes in many layers. The regular spacing between peaks in figure 4 corresponds to the bilayer thickness, and this shows that the U/Gd multilayers form coherent superlattices. The fact that these peaks are rather broad indicates that the coherence extends over only a few bilayers. We were unable to obtain consistent parameter sets in fits of the models of Fullerton *et al* [18] or Jehan *et al* [19]. We therefore employed the approximation of using the two principal diffraction peaks to estimate the individual lattice spacings of the U and Gd layers.

Figure 5 summarizes the lattice spacing values as determined from the x-ray diffraction profiles for a number of U/Gd samples. The upper panel presents the variation of d_{Gd} as a function of t_{Gd}, whereas the lower panel shows d_U as a function of both t_{Gd} and t_U. It was not possible to distinguish the gadolinium diffraction peak positions in the case of varying t_U, since the gadolinium layers were too thin to give an appreciable diffracted intensity.

As described earlier, the lattice parameter in a sputtered film (thickness 500 Å) of Gd (2.920 Å) is larger than that of bulk Gd (2.899 Å); these values are noted in figure 5. For multilayers containing thin gadolinium layers the Gd lattice is further expanded, but contracts towards the sputtered thin film value as the layers become thicker. There is little observable change in the U lattice spacing, d_U, as t_U is varied. For the case of these samples the gadolinium layer thickness is constant at 20 Å. However, a slight expansion of the lattice is observable for thick U layers. An interesting result observed here is the dependence of d_U upon the gadolinium layer thickness, with $t_U \sim 26$ Å. A consideration of the lattice parameter sizes of the hcp Gd and U phases, reveals a likely strain acting to expand the U lattice. The trend observed in figure 5 implies an increase in the strain acting on the U layers, as t_{Gd} is increased, which provides a mechanism for the observed increase in d_U.

4. Conclusions

The x-ray reflectivity spectra of all samples display well-defined Bragg peaks, which give accurate determinations of the bilayer thickness. The thicknesses of the individual layers are then obtained by maintaining consistency across a range of measurements. The inclusion of niobium buffer and capping layers has considerably reduced the complexity of the structural model required to simulate the reflectivity spectra of previous samples [7].

The situation in the case of the U/Gd system is significantly different. An intense diffraction peak is present that does not correspond to any known for α-U, but at a position close to that reported for a novel hcp phase of uranium [16]. The lattice spacing, d_U, determined by this peak for thick U layers is about 2.80 Å and does not change significantly as the U layer thickness is varied (for constant t_{Gd} of 20 Å). This gives a c-axis lattice parameter for hcp uranium of 5.60 Å, somewhat larger than values put forward in the study of uranium grown on tungsten [16]. Assuming the same atomic volume of 20.7 Å^3 for hcp U as that for α-U and taking the c-axis parameter determined from x-ray diffraction measurements, the resulting a-axis value is 2.91 Å, giving a c/a ratio close to 1.9, much larger than that expected from a hard sphere model of the crystal structure. The lattice parameter of the a-axis also represents the U–U nearest neighbour distance in the hcp crystal structure, which in the α-U phase is 2.75 Å. A comparison of the local environments of U atoms in these two structures reveals a major change in the coordination and a lattice expansion of $\sim$2.5%. The observation of such intense diffraction spectra is then remarkable. The mismatch, between the Gd ($a = 3.56$ Å for the sputtered film) and hcp U ($a \sim 2.91$ Å) is about 22%, yet growth along the common c-axis remains good.

In summary, these experiments have shown that U/TM (TM = Fe and Co) multilayers are difficult to grow with sharp interfaces, and efforts to use sapphire rather than glass [7, 8] have failed to reduce the interfacial roughness. We suggest these problems are due to the large misfit in size between U and the TM elements. In the U/Gd multilayers, despite a large size difference, the structural quality is much better. For large Gd layer spacings considerable roughness is observed, which suggests Gd columnar growth. Of particular importance is that the U/Gd multilayers contain uranium in a novel hexagonal close packed (hcp) form, which does not exist in the bulk, nor is it found in multilayers of U with hcp-Co. This result motivates an effort to prepare epitaxial films of hcp uranium and examine its properties.

Acknowledgment

RS acknowledges the receipt of an EPSRC research studentship.

References

[1] Bland J A C and Heinrich B 1994 *Ultrathin Magnetic Structures I* (Berlin: Springer)
[2] Severin L, Nordström L, Brooks M S S and Johansson B 1991 *Phys. Rev.* B **44** 9392
[3] Fumagalli P, Plaskett T S, Weller D, McGuire T R and Gambino R J 1993 *Phys. Rev. Lett.* **70** 230
[4] Kernavanois N, Mannix D, Dalmas de Réotier P, Sanchez J P, Yaouanc A, Rogalev A, Lander G H and Stirling W G 2004 *Phys. Rev.* B **69** 54405
[5] Fumagalli P, Plaskett T S, McGuire T R, Gambino R J and Bojarczuk N 1992 *Phys. Rev.* B **46** 6187
[6] Rosa M A, Diego M, Alves E, Barradas N P, Godinho M, Almeida M and Gonçalves A P 2003 *Phys. Status Solidi* a **196** 153
[7] Beesley A M *et al* 2004 *J. Phys.: Condens. Matter* **16** 8491
[8] Beesley A M *et al* 2004 *J. Phys.: Condens. Matter* **16** 8507
[9] Wilhelm F *et al* 2007 *Phys. Rev.* B **76** 024425
[10] Brown S D *et al* 2003 *J. Appl. Phys.* **93** 6519
[11] Hellwig O, Song G, Becker H W, Birkner A and Zabel H 2000 *Mat.-wiss. u. Werkstofftech.* **31** 856
[12] Névot L and Croce P 1980 *Rev. Phys. Appl.* **15** 761
[13] Langridge S http://www.rl.ac.uk/largescale/
[14] Springell R, Zochowski S W, Ward R C C, Wells M R, Brown S D, Bouchenoire L, Wilhelm F, Langridge S, Stirling W G and Lander G H 2008 *J. Phys.: Condens. Matter* **20** 215230
[15] Patterson A L 1939 *Phys. Rev.* **56** 978
[16] Berbil-Bautista L, Hänke T, Getzlaff M, Wiesendanger R, Opahle I, Koepernik K and Richter M 2004 *Phys. Rev.* B **70** 113401
[17] Molodtsov S L, Boysen J, Richter M, Segovia P, Laubschat C, Gorovikov S A, Ionov A M, Prudnikova G V and Adamchuk V K 1998 *Phys. Rev.* B **57** 13241
[18] Fullerton E E, Schuller I K, Vanderstraeten H and Bruynseraede Y 1992 *Phys. Rev.* B **45** 9292
[19] Jehan D A, McMorrow D F, Cowley R A, Ward R C C, Wells M R, Hagmann N and Clausen K N 1993 *Phys. Rev.* B **48** 5594